The sharpness of the (111) reflection was due to the absence of chemical gradients within the phase. As diffusion occurred, the (111) reflection of the second α phase only decreased in intensity as a function of time with no shifting to lower 2θ values. The sharpness of the (111) reflection of the Cu rich α phase was also invariant. In the case of sample Pd-Cu-2, the XRD reflections of the Cu rich α phase were observed for two hours. Only a Pd rich α phase was observed after a total annealing time of 5 hr at 650ºC. Figure 7-5(b) shows the XRD patterns collected while decreasing the temperature from 650 to 300ºC at a cooling rate of 3ºC/min. The ordered β phase nucleated at a temperature higher than 525ºC and grew at the expense of the initially present α phase.

The XRD pattern of sample Pd-Cu-2 face 1 at room temperature showed essentially β phase and a small amount of α phase as seen in Figure 7-6. However, the XRD pattern of face 2 of sample Pd-Cu-2 at room temperature, also in Figure 7-6, showed essentially α phase and a small amount of β phase. EDX analysis across the Pd-Cu alloy in face 1 and face 2 indicated a Cu concentration, within the volume irradiated by electrons (0.5-1 μm in thickness), higher in face 1 than in face 2 by 4 wt% as seen in Figure 7-7. Figure 7-7 also shows that even after an annealing time of five hours at 650ºC a uniform Pd-Cu alloy was not reached. In fact the Pd content below the volume irradiated by X-rays (from 0 to 3 μm in Figure 7-7) is higher than 70 wt% in both faces indicating the presence of the α phase. Therefore, sample Pd-Cu-2 face 1 had a structure consisting of 3 μm thick Pd-rich α phase and 3μm thick β phase. Sample Pd-Cu-2 face 2 was essentially consisting of a Pd-rich α phase.

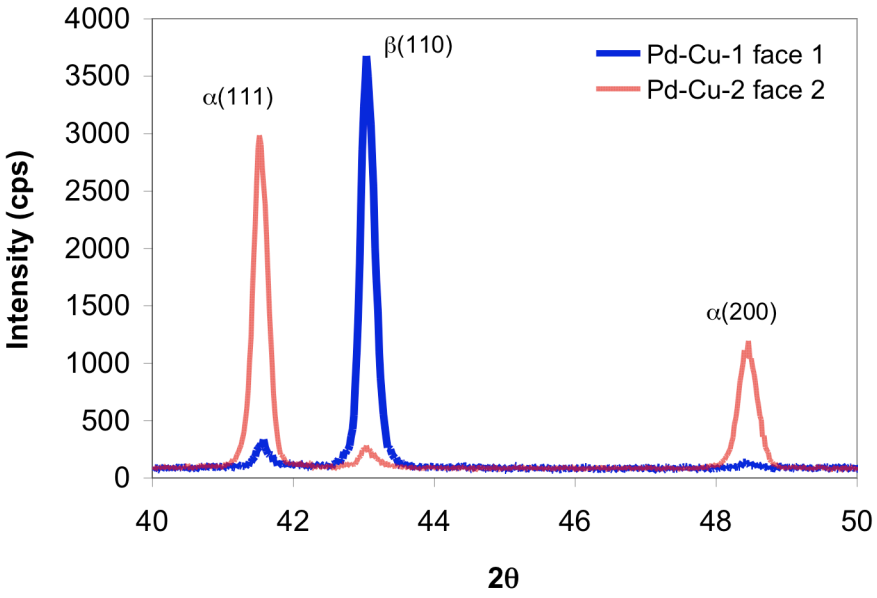

Figure 7-6 XRD patterns of sample Pd-Cu-2 face 1, mainly β phase, and face 2 mainly α phase

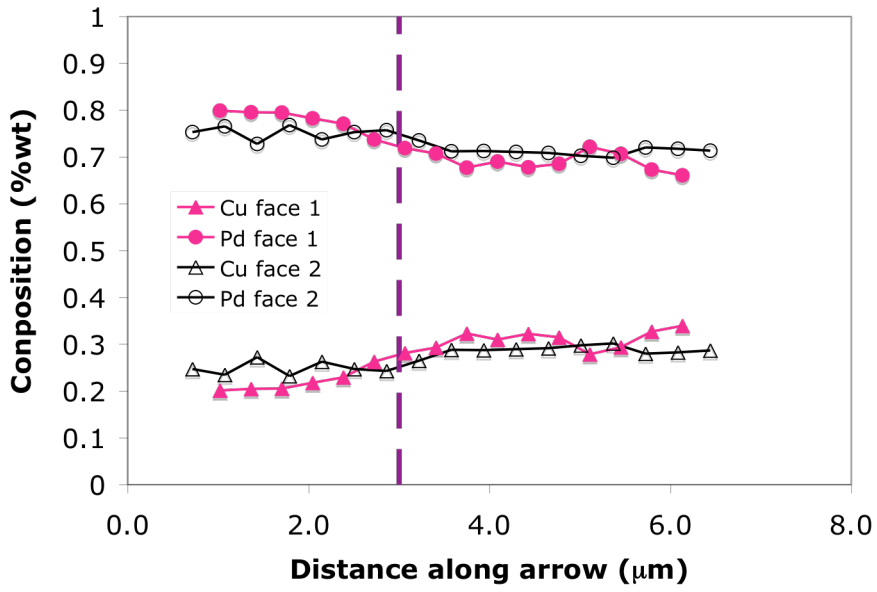

Figure 7-7 Elemental composition across the thickness of sample Pd-Cu-2 after heat-treatment for face 1 and face 2. The dashed line represents the penetration of X-rays at an angle of 2θ=40°

This example showed that a difference in Cu concentration of only 4 wt% led to a completely different structure in Pd-Cu alloys. Also, according to the Pd-Cu phase diagram[1], it is crucial to target a Cu concentration of exactly 42 wt% if the β phase is desired in the 450-500ºC temperature range.

Figure 7-8 shows the phase changes as a function of time at 650ºC, as well as XRD patterns during quench and dwell at 525ºC of sample Pd-Cu-3. The very first pattern was mainly pure Pd and pure Cu phases. However the second pattern already included, after a short time, two α phases similar to the two α phases seen during the annealing of sample Pd-Cu-2. The first α phase, initially Cu rich with the (111) reflection exiting at 2θ ca. 42°, was characterized by very broad peaks due to concentration gradients. As diffusion occurred the peaks of the Cu rich phase shifted from values of 2θ ca. 42° to values of 2θ ca. 41° indicating the progressive Pd enrichment.

[1] The Pd-Cu phase diagram is shown in Figure 7-14, page 196

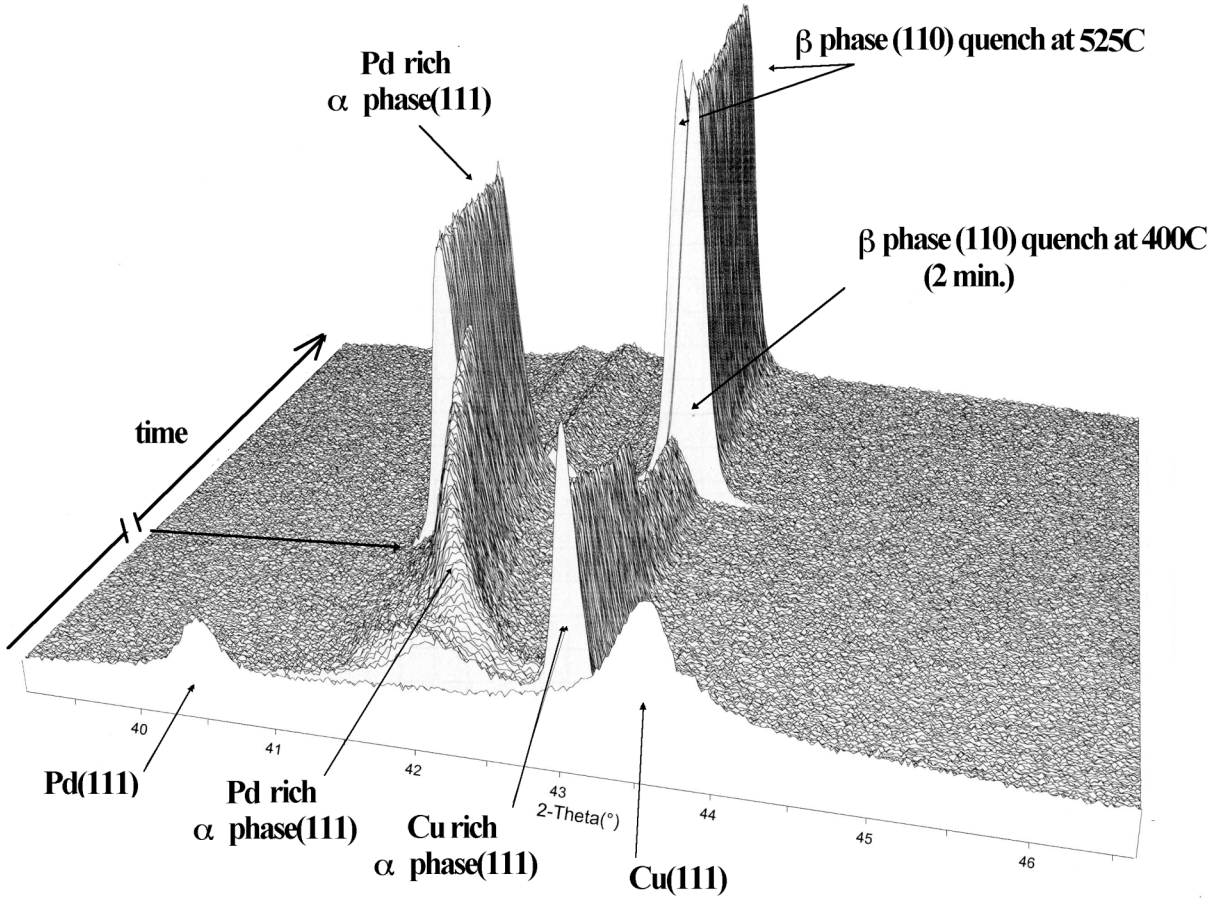

Figure 7-8 XRD pattern collection of sample Pd-Cu-3 during heat-treatment. Part of the pattern for the homogenization process was eliminated in the 3D spectra collection.

Moreover, peaks sharpened and increased in intensity as a function of time indicating the growth of a Pd rich phase. The second α phase, very rich in Cu and characterized by a very sharp (111) reflection, behaved the same way as in sample Pd-Cu-2. That is, the (111) reflection peaks only decreased in intensity with neither shifting towards Pd rich side nor changes in sharpness. The decrease in intensity indicated the dissolution of the Cu rich α phase with time.

After 5 hr at 650ºC, the sample was quenched to 400ºC (the sample was brought from 650°C to 400°C in less than 1 min.) and stayed at 400°C for 2 minutes. The β phase, with its characteristic (100) reflection at 2θ ca. 43°, nucleated within 30 seconds. It can be seen that some of the parent phase still remained. After 2 min at 400ºC, the sample was heated up to 525ºC to trigger the β to α transformation. No decrease in intensity of the β peak was seen for two hours indicating that at that particular Cu concentration, the β phase was stable at temperatures equal to or below 525ºC. Also, no increase in the intensity of the remaining α phase was seen. Therefore it appeared that the Cu concentration of the volume irradiated by X-rays was higher than or equal to 42 wt%.

The peaks seen on sample Pd-Cu-3 corresponding to the α phase might have been due to the Cu concentration gradient across the thickness. The XRD pattern of sample Pd-Cu-3 face 1 at room temperature showed essentially β phase and a slight amount of α phase (Figure 7-9). The XRD pattern of sample Pd-Cu-3 face 2 at room temperature only showed β phase. EDX analysis across the Pd-Cu alloy in face 1 and face 2 indicated a Cu concentration, within the volume irradiated by X-rays, were very similar as seen in Figure 7-10.

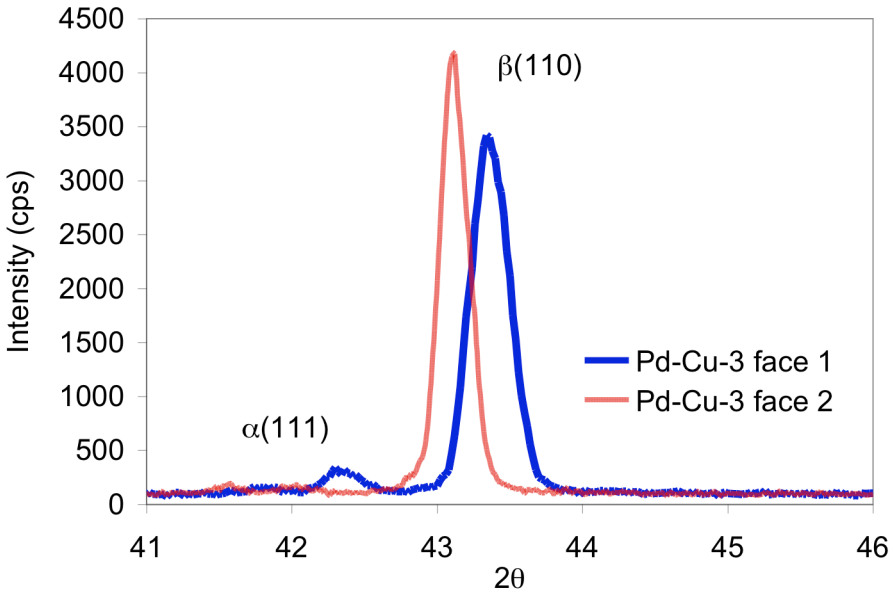

Figure 7-9 XRD patterns of sample Pd-Cu-3 face 1 and 2

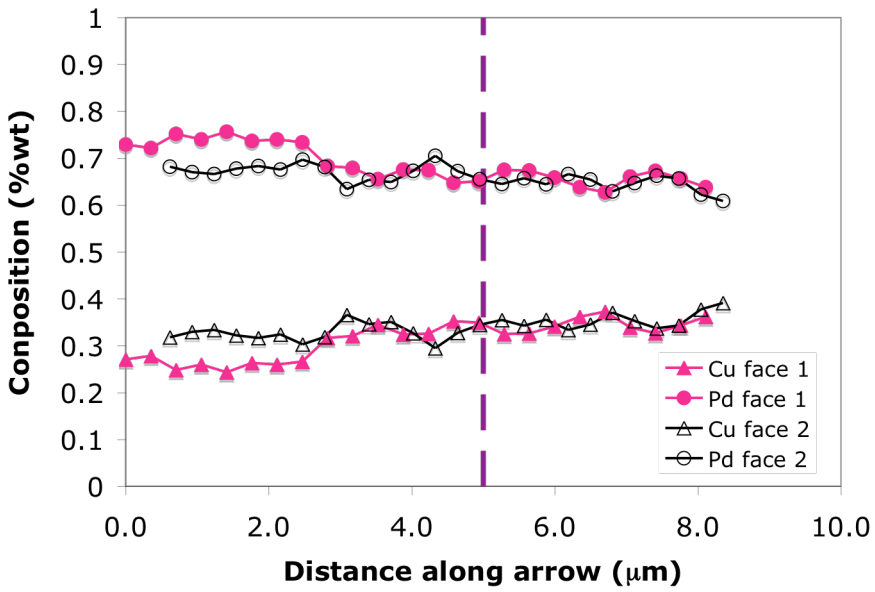

Figure 7-10 Elemental composition across the thickness of sample Pd-Cu-2 after heat-treatment for face 1 and face 2. The dashed lined represents the penetration of X-rays at an angle of 2θ=40°

Figure 7-10 also shows that even after an annealing time of five hours at 650ºC a uniform Pd-Cu alloy was not reached. In fact the Pd content below the volume irradiated by X-rays (from 0 to 3 μm in Figure 7-10) was higher than 70 wt% in both faces indicating the presence of the α phase.

Figure 7-11(a) shows the surface of sample Pd-Cu-1 after heat-treatment and accidental slight oxidation. It is important to note that even after quenching (from 800°C to room temperature in less than a minute) neither cracking of the membrane nor peeling from the support occurred, which is in agreement with the reported mechanical robustness of the Pd-Cu alloy (McKinley, 1967). Particularly, Mc Kinley, (1967) observed no wrinkles or distortions in Pd-40wt% Cu cycled ten times between 350°C and room temperature. Pure Pd underwent severe distortions after similar treatment.

Figure 7-11 (b) shows the morphology of sample Pd-Cu-2 after heat-treatment. Several pinholes were presented on the surface, which were formed by metal particles aggregation (sintering) due to the high temperatures used. The SEM micrograph of sample Pd-Cu-1, Figure 7-11(a), did not show any pinholes. The thin oxide layer, accidentally formed, could have covered the pinholes. A very uniform alloy was also seen after heat-treatment. Figure 7-11 (c) is an SEM photograph of sample Pd-Cu-3 after the described heat-treatment. The surface of the alloy showed light and dark regions. Numerous pinholes were seen. The absence of cracks in the Pd-Cu layers even after rapid cooling and heating demonstrate the robustness of the alloys, however, the surface of all samples was characterized by numerous pinholes after heat-treatment.

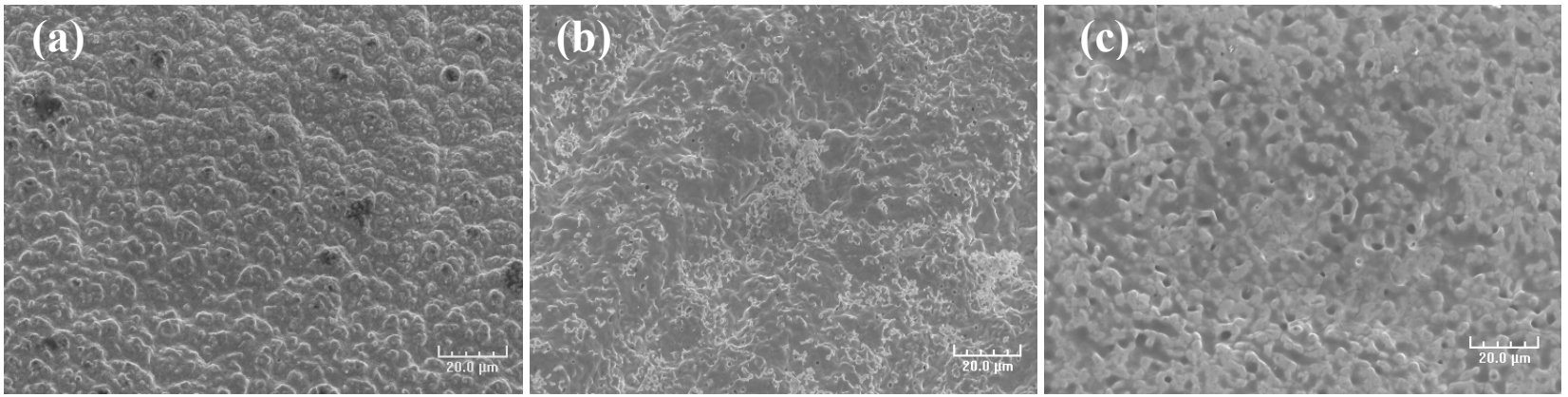

Figure 7-11 SEM picture of sample Pd-Cu-1 (a), sample Pd-Cu-2 (b) and sample Pd-Cu-3 (c) after heat-treatment

.

The formation of pinholes is detrimental to membrane selectivity therefore, it appeared, as expected, that a temperature of 650ºC was too high for alloying these bimetallic layers.

According to the Pd-Cu phase diagram, page 196, only a disordered fcc phase is stable at temperatures higher than 600°C regardless of the Cu concentration. Therefore, during annealing of bimetallic layers only one fcc phase with very broad peaks should be seen assuming that, at the initial stage of the treatment, some Cu diffused into the Pd and some Pd diffused into the Cu. However, two phases were seen in the case of sample Pd-Cu-2 and sample Pd-Cu-3. Particularly, the sharpness of the Cu rich fcc phase (111) reflection indicated that its composition hardly changed as a function of time, only the relative quantity (or thickness) decreased. Therefore, the alloying process of a Pd-Cu bimetallic layer took place across the interface that separated the Pd rich phase from the very rich Cu phase. As diffusion occurred, Cu atoms diffused into the Pd rich phase through the interface faster than Pd atoms diffused into the Cu rich phase. The diffusion of Cu within the Pd rich phase was relatively fast since the Pd rich phase originally showed broad peaks (Cu gradients across the thickness of the Pd rich phase) but sharpened at the end of the annealing process. Schematically, the alloying process of Pd-Cu bi-layers took place as if a Cu layer, analog to a Cu atoms reservoir, disappeared at the expense of a Pd rich phase. The diffusion of Cu through the Cu/Pd-Cu interface led to the shifting of the Cu/Pd-Cu interface in the outer direction. The above-described alloying process is in agreement with results reported by Ma et al. (2004). Figure 7-12(a), shows the cross-section of a 12μm Pd-12μm Cu bimetallic layer annealed at 500°C for 120 hr from Ma et al. (2004).

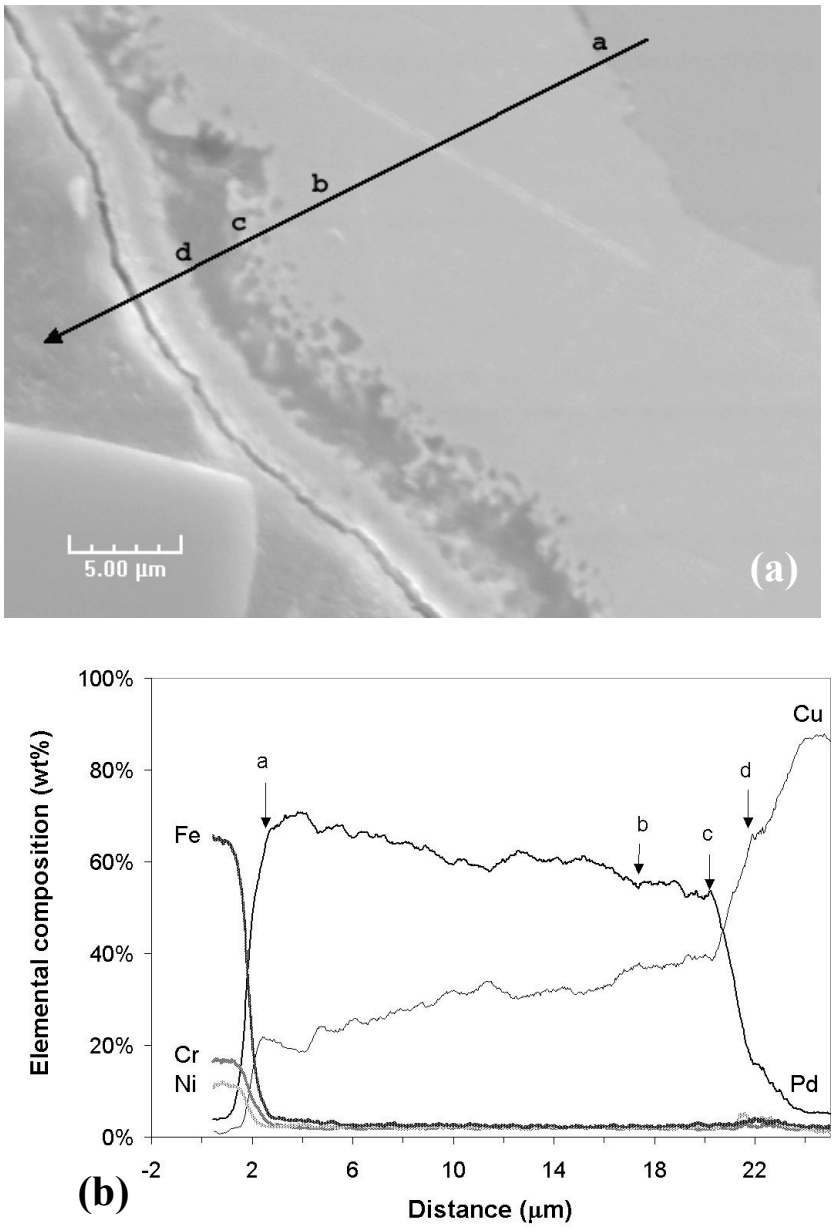

Figure 7-12 (a) SEM micrograph (b) Composition profile of different elements along the arrow in by EDX line scan.

The annealing conditions were not the same, however, the analysis of the composition across the membrane revealed a very rich Cu layer, >80wt% in Cu, starting at point d. Underneath the rich Cu layer a dark layer appeared between points c and d, which was the Cu/Pd-Cu interface layer. The Pd rich phase, a-c region in Figure 7-12(b), would certainly appear as the Pd rich phase with broad peaks at the beginning of the annealing procedure, though sharper at the last stages due to the fast diffusion of Cu within that phase. The Cu rich layer starting at point d, was the Cu atoms reservoir leading to the sharp peaks and the barrier c-d shifted from the initial interface at 12μm outwards due to the incorporation of Cu atoms from the reservoir by Pd-rich phase.

7.4.2 The nucleation and growth of the β phase

The nucleation of the ordered β phase took place instantaneously at 400°C when sample Pd-Cu-3 was quenched from 650°C. The α to β transformation is theoretically accompanied by a shrinkage in the lattice parameter form ca. 0.3758 nm to ca. 0.2977 nm, which represents a contraction of 21% of the initial lattice. The fast change in lattice parameter leads to the cracking of thin supported Pd-Cu layer. The nucleation of the ordered β phase can be better controlled by slowly decreasing the temperature to the operating temperature such as in sample Pd-Cu-2.

The nucleation and growth of the β phase was studied in great detail with sample Pd-Cu-4. Sample Pd-Cu-4 had a theoretical Cu concentration of 40 wt%. The sample was held at 650ºC in He atmosphere until the peaks of the disordered fcc α phase were visible. The sample was quenched to 550ºC and the nucleation and growth of the β phase were followed as a function of time at 550ºC. After a given dwell time (10-90 min.) at 550ºC the temperature was brought up to 650ºC to re-dissolve the formed β phase. After

30 min at 650ºC the sample was quenched again to 500ºC and the nucleation and growth of the β phase was followed as a function of time. The dissolution at 650ºC-quenching procedure was performed at 550, 500, 450, 400, 350 and 300ºC. The β phase dissolution was always performed at 650ºC for 30 min. The dwell time at a given temperature was 10-15 minutes during the first experiment (Pd-Cu-4a) and 1-1.5 hr during the second experiment (Pd-Cu-4b). Both experiments were performed with the same sample Pd-Cu-4. Figure 7-13 shows $X_\beta / X_{\beta,\,equilibrium}$ as a function of time at 550, 500, 450, 400, 350 and 300ºC after quenching from 650ºC. The transformation path was also plotted in the Pd-Cu phase diagram as seen in Figure 7-14.

Figure 7-13 shows $X_\beta / X_{\beta,\,equilibrium}$ as a function of time at 300, 350, 400, 450, 500 and 550ºC after rapid cooling from 650ºC. The ordering transformation fcc → bcc that took place when quenching the sample from 650ºC to any given temperature was limited by diffusion at 300, 350 and 400ºC. At 300, 350 and 400ºC the initial percentage of β phase was equal to 0.3 due to the nucleation and growth that took place during the 2 minutes needed to cool the sample from 650ºC to 300, 350 and 400ºC. The diffusion was so sluggish at 300ºC that the β phase did not grow. At 350 and 400ºC the transformation rate increased even though the transformation appeared to be limited by diffusion. At 450ºC the rate of transformation was the fastest and decreased as the quenching temperature was increased due to thermodynamic limitations. Figure 7-14 shows the ordering transformation path after 15 seconds and 10 minutes within the Pd-Cu phase diagram. The 10 minutes lines starts to curve to the right at 450ºC indicating that for temperatures lower than 450ºC the diffusion of metal atoms was the limiting process.

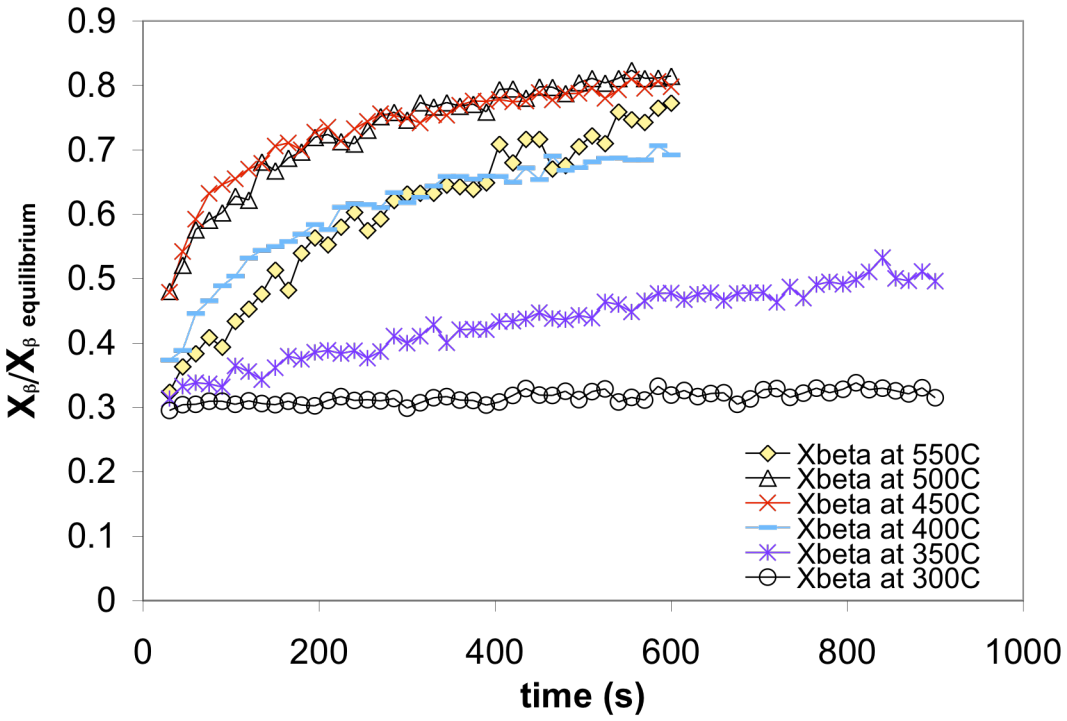

Figure 7-13 X_β as a function of time at different temperatures after quenching from 650°C

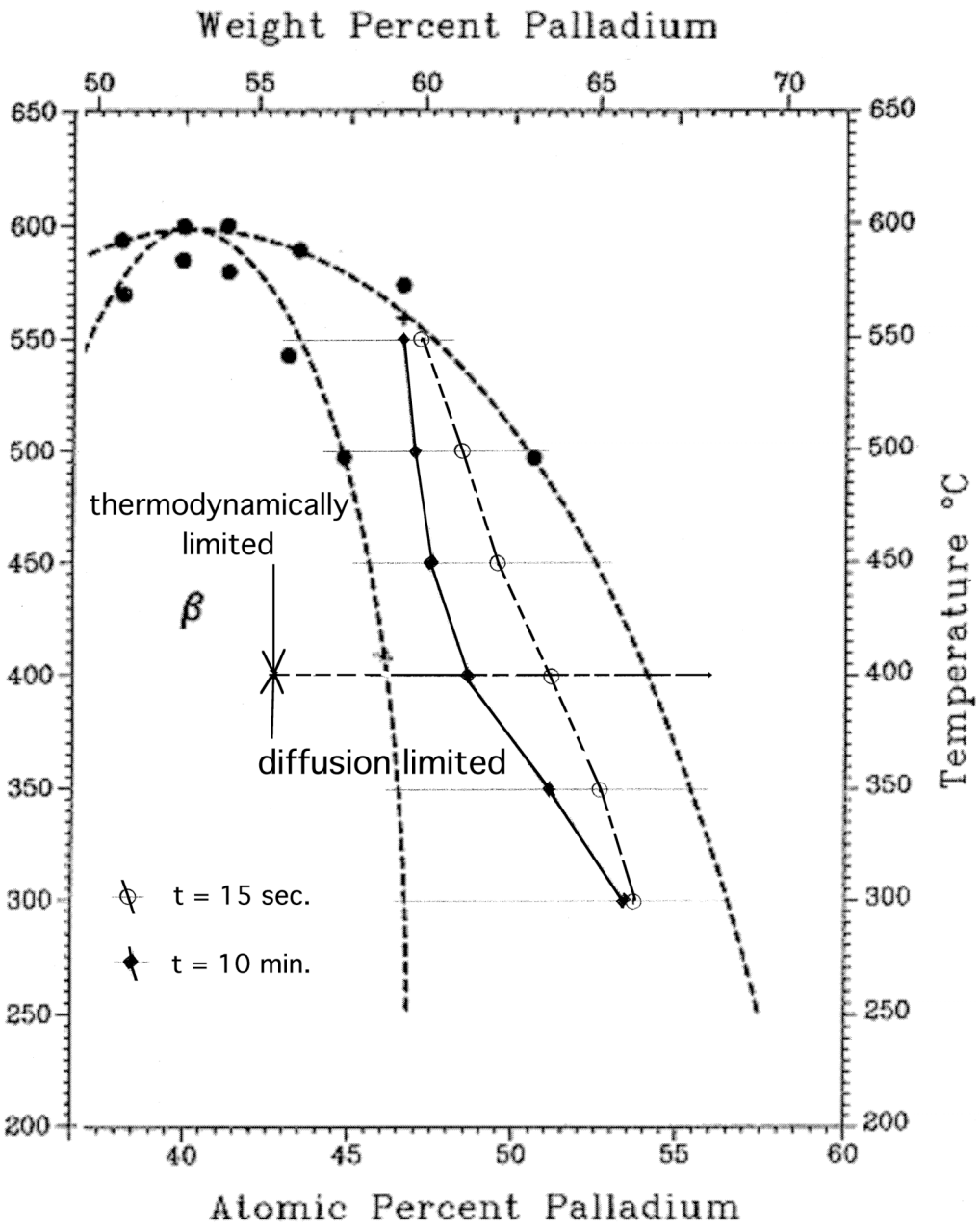

Figure 7-14 phase transformation path at different times t=0 sec and t=10 min

In order to better elucidate the ordering transformation the sample was held for longer times, 1 – 1.5 hr, at 400, 450, 500 and 550ºC. The ordering transformation is plotted during the first 200 seconds in Figure 7-15(a) for all temperatures. The cooling rate from 650 to 450 and 400ºC was very fast although some β phase nucleated and grew during the time, 1-2 min., it took to "quench" the sample. Hence, the β phase percentage at t=0 did not equal 0 but 0.28 as pointed by the black arrow. Also the curves at 400 and 450ºC are characterized by an inflection point indicating that the initial β phase concentration due to the cooling was taken over by the β phase growth that really happened at those temperatures. Hence, the first data point at 450ºC was neglected as well as the two first data points at 400ºC.

Figure 7-15(b) shows the ordering transformation in the 0-3600 sec. time interval. The ordering transformation was characterized by a sharp nucleation and growth during the first 200 sec. an intermediate regime between 200 and 1000 sec. and a linear increase with time after 1000 sec. As seen in Figure 7-16(a) and (b) the ordering transformation, even though it was a "nucleation and growth" transformation, could not be fitted with either an Avrami model or a quadratic model. When the experimental data were fitted with the Avrami model, time exponents close to 0.2-0.5 were found (see Figure 7-16(a)), which were not proper of usual time exponent values found in metals i.e. 3-4. When the experimental data were fitted with a quadratic model, no linear relation could be found for the $X_\beta / X_{\beta,\,equilibrium}$ vs. $t^{0.5}$ data points. However at times higher than 1000 sec. the growth of the β phase was considered as linearly dependent on √t.

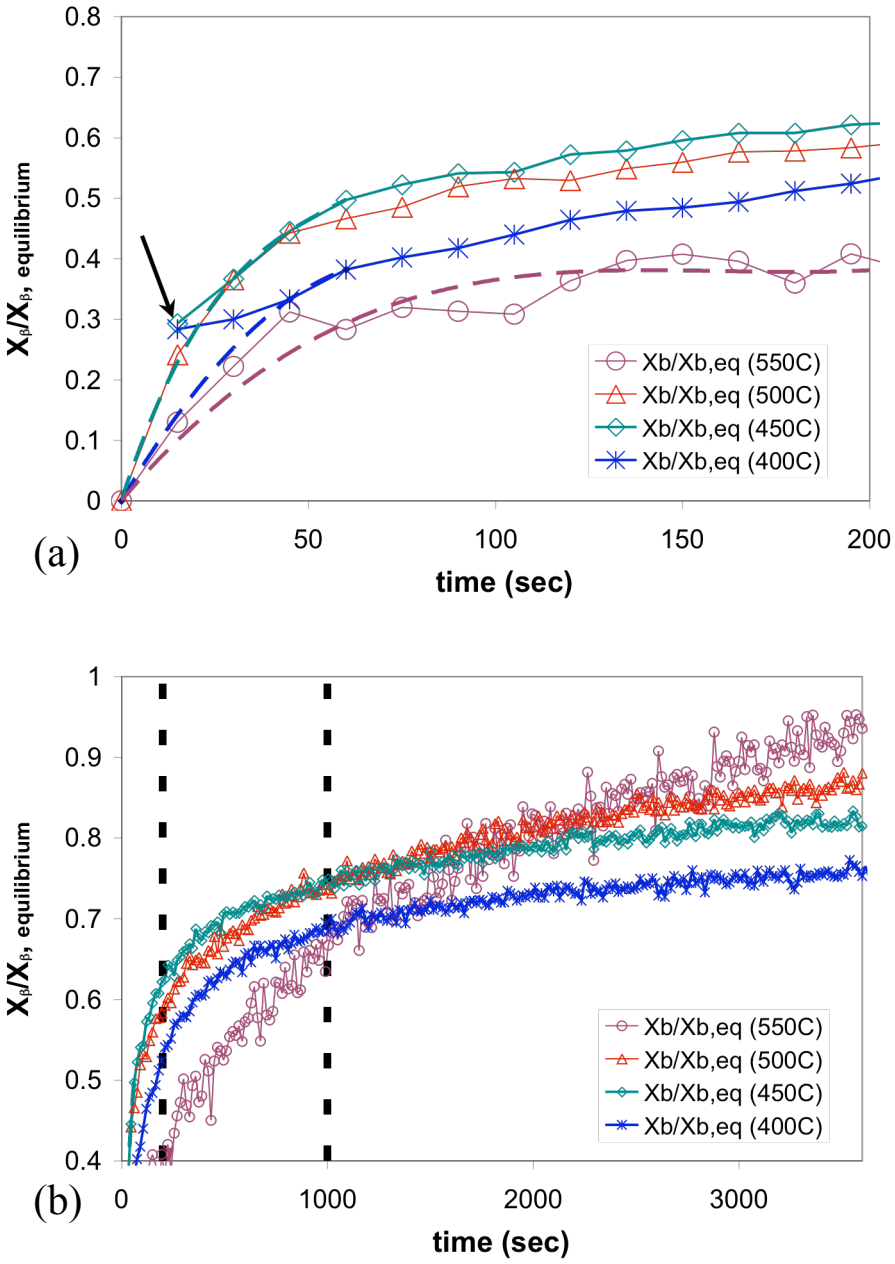

Figure 7-15 (a) fcc → bcc ordering transformation in the 0-200 sec. time range. (b) ordering transformation in the 0-3600 sec time range

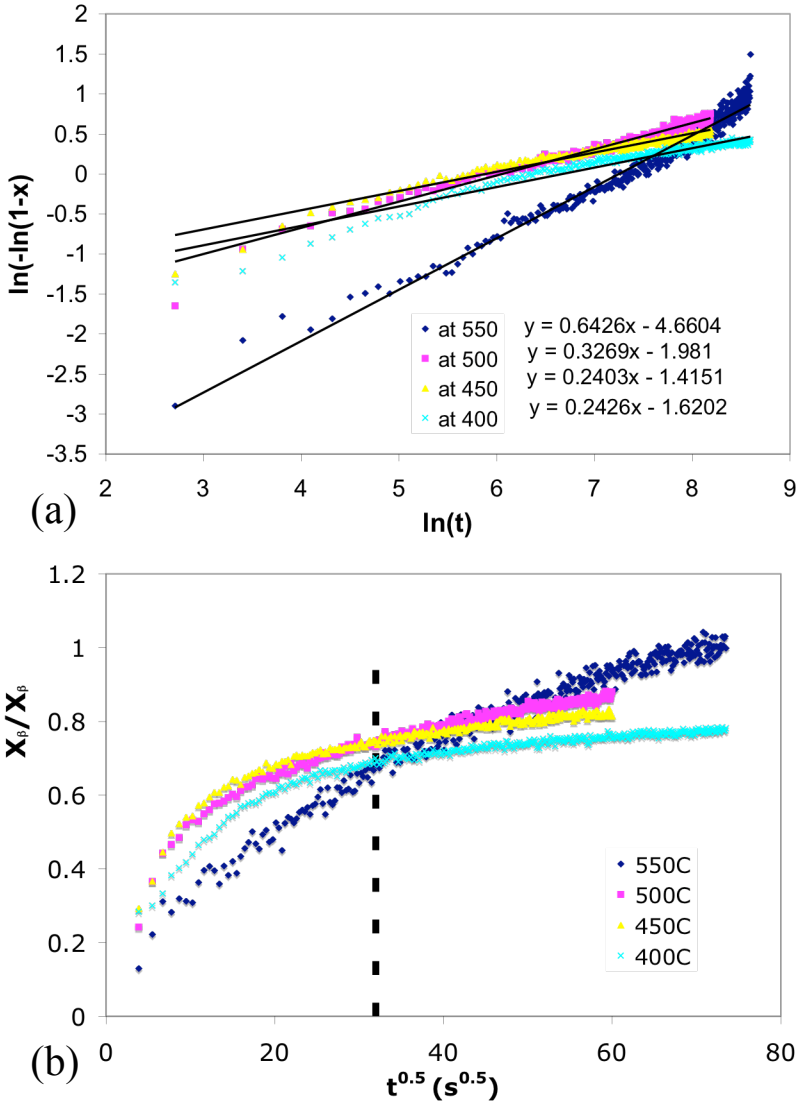

Figure 7-16 (a) Avrami model (b) quadratic model

The kinetics of this ordering transformation was therefore studied by determining the initial transformation rates at t=0 sec and the growth rates between 1000 and 3000 sec.

In order to calculate the initial rates, the experimental $X_{\beta}/ X_{\beta, \text{equilibrium}}$ vs. time functions were interpolated between 0 and the first 10 data points neglecting the first datum point at 450ºC and omitting the two first data points at 400ºC (see Figure 7-15(a)). Interpolation curves are shown with dashed lines in Figure 7-15(a). The initial rate was given by the tangent at *t*=0 sec. The growth rate between 1000 and 3000 sec was assumed to be linear with time. Figure 7-17 shows the Arrhenius plot of the initial rates and $r_{1000\text{-}3000}$ rates.

As already found for the first experiment, a maximum initial rate was found at 400-450ºC. At times higher than 1000 sec. the activation energy for the ordering transformation was 40kJ mol^{-1}. The activation energy for Pd-Cu inter-diffusion is in the order of 200kJ mol^{-1}, therefore, it appeared that the rate-limiting step for the ordering transformation was not diffusion.

In fact, as seen in Figure 7-15(b), it appeared that the rate at which the β phase fraction reached its equilibrium value ($X_{\beta, \text{equilibrium}}$) was independent of the temperature. Several studies pointed out the ordering fcc → bcc transformation had a bainitic or a martensic character. The transformation path was also plotted in the Pd-Cu phase diagram as seen in Figure 7-18

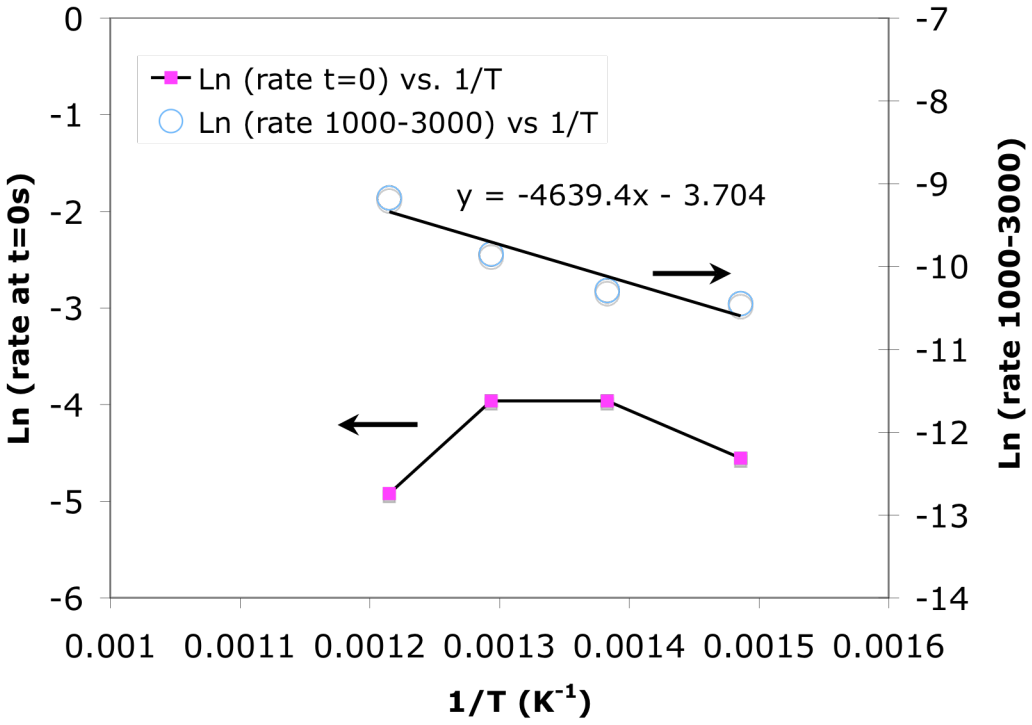

Figure 7-17 Ln (rate t=0 sec) and Ln (rate 1000-3000 sec) as a function of 1/T

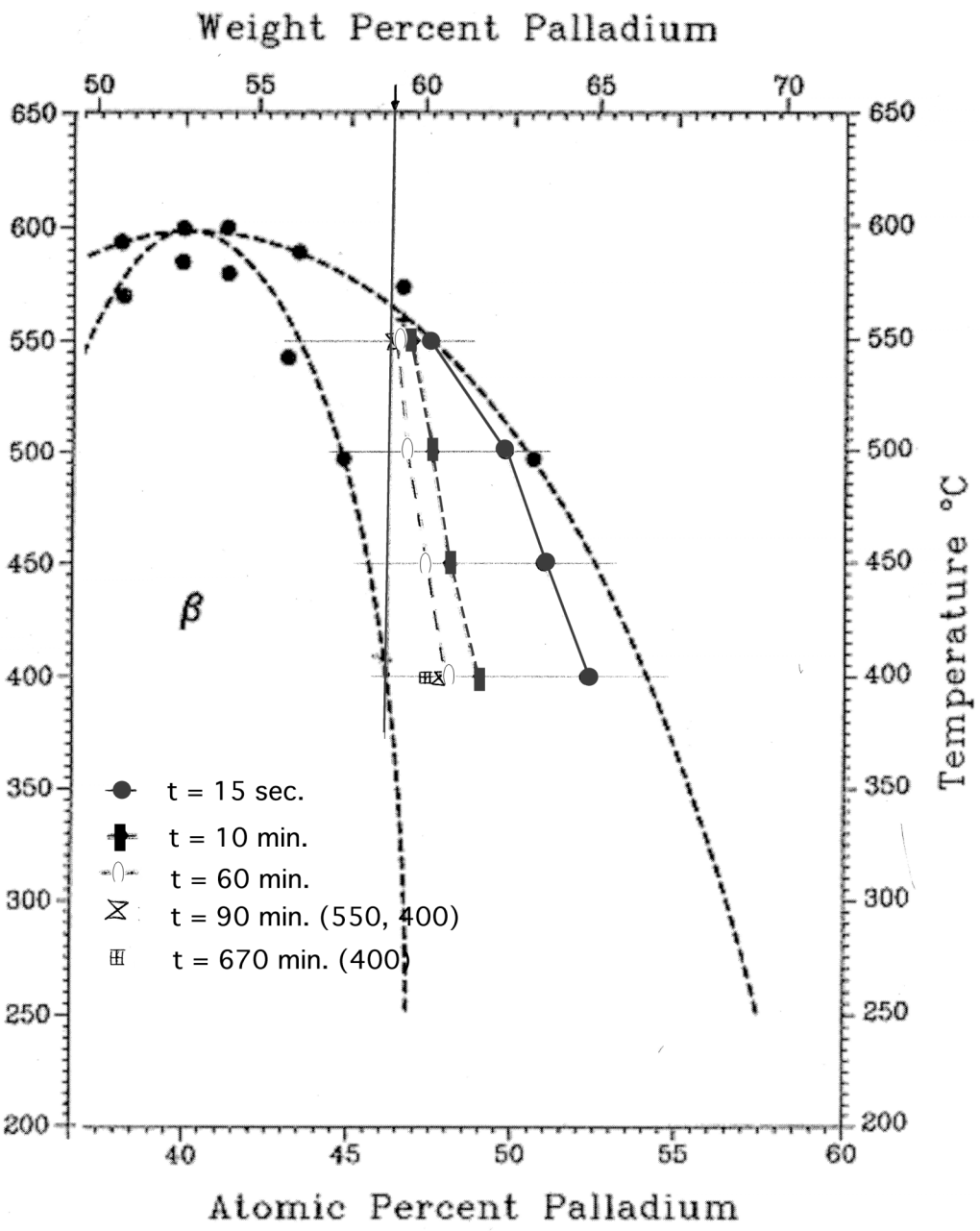

Figure 7-18 Phase transformation path at different times t=0 sec, t=10 min

7.4.3 H_2 permeation through a composite Pd-Cu membrane

The H_2 permeance of Ma-41 was measured at 250, 300, 350, 400 and 450ºC. As seen in Figure 7-19, no decline in H_2 permeance was observed at 450ºC for over 500 hr indicating that no intermetallic diffusion occurred for temperatures below or equal to 450ºC

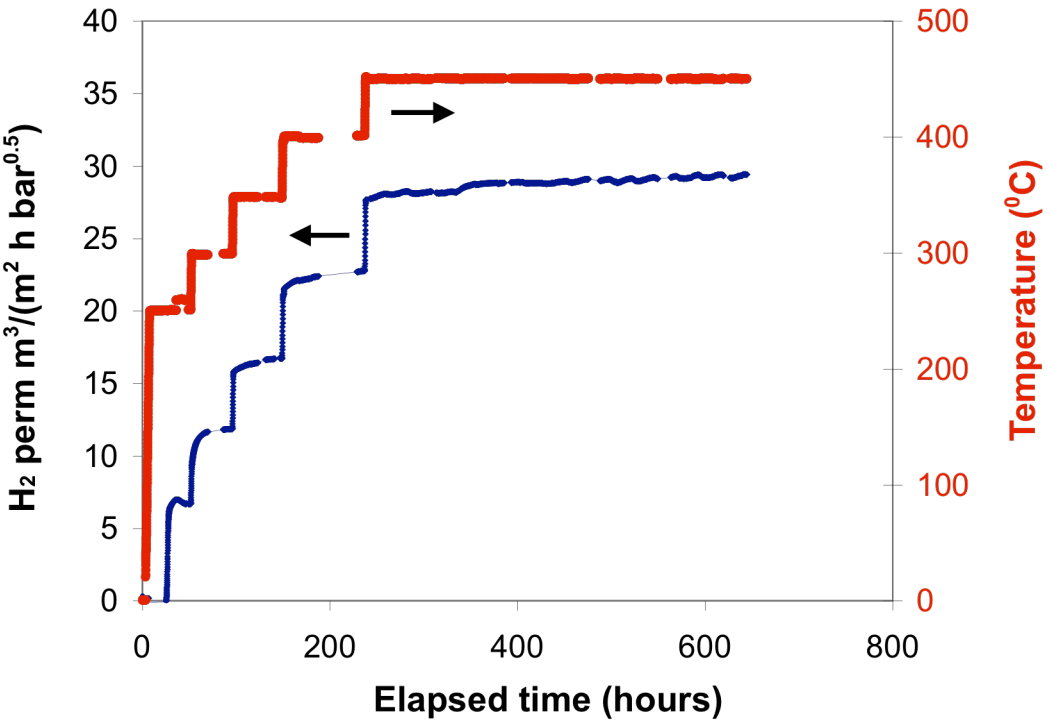

Figure 7-19 Long term H_2 stability for Ma-41 membrane.

Figure 7-20 shows the H_2 flux of Ma-41 membrane as a function of $\Delta(P^{0.5})$ at 250, 300, 350, 400 and 450ºC. When the H_2 flux data in Figure 7-20 were fitted by adjusting the n-exponent with Equation (3-3), the n-exponent was equal to 0.57-0.58 ±0.1 indicating that assuming Sieverts' law was valid. Moreover, the value of the ξ_{250} parameter for the graded support of Ma-41 was estimated to be higher than 40, therefore, deviations from Sieverts' law at high temperatures due to mass transfer resistance were negligible. Hence, the H_2 flux was consider as a linear function of $\Delta(P^{0.5})$ and bulk diffusion was the rate-limiting step. The flux data in Figure 7-20 were then fitted with Equation (3-2) to determine the H_2 permeance, $F_{0.5}$. Figure 7-21 shows the values of the H_2 permeance, $F_{0.5,}$ of membrane Ma-41 in an Arrhenius type of plot. The activation energy for H_2 permeation based on $F_{0.5}$ values determined after long annealing times equaled 20.6 kJ/mol. The activation energy for H_2 permeation was also determined by measuring H_2 flux as the temperature was changed at a rate of 1ºC/min. During each temperature change, an average of 15 (H_2 flux, Temperature) data points were recorded. The H_2 permeance, F_{H2}, was then determined using Equation (3-1). $Ln(F_{H2})$ vs. 1/T for each of the 250-300, 300-350, 350-400 and 400-450ºC temperature changes was plotted in Figure 7-21. For each temperature change the activation energy was determined and plotted in Figure 7-22. The activation energy for H_2 permeation, F_{H2}, was equal to 17.1 $kJmol^{-1}$ in the 300-350 temperature window and 15.6 $kJmol^{-1}$ in the 400-450ºC temperature range. The activation energy for H_2 permeation was higher when considering $F_{0.5}$ after long annealing periods than when considering F_{H2} during the different temperature changes. The difference was due to the fact that at all temperatures the H_2 permeance slightly increased over time as the alloying process took place as explained in Section 3.2.4. The increase in H_2 per-

meance was not due to leaks since the selectivity (H_2/He) of this membrane was well above 300 at all temperatures.

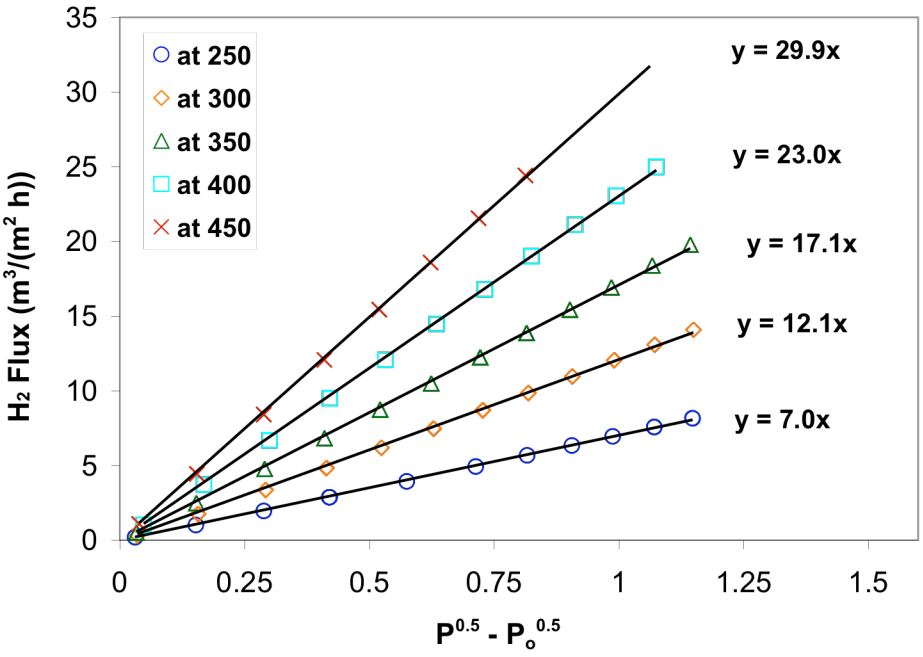

Figure 7-20 H_2 flux at 250-450°C for Ma-41 membrane as function of Sieverts' driving force. Numbers beside experimental lines are the H_2 permeance $F_{0.5}$.

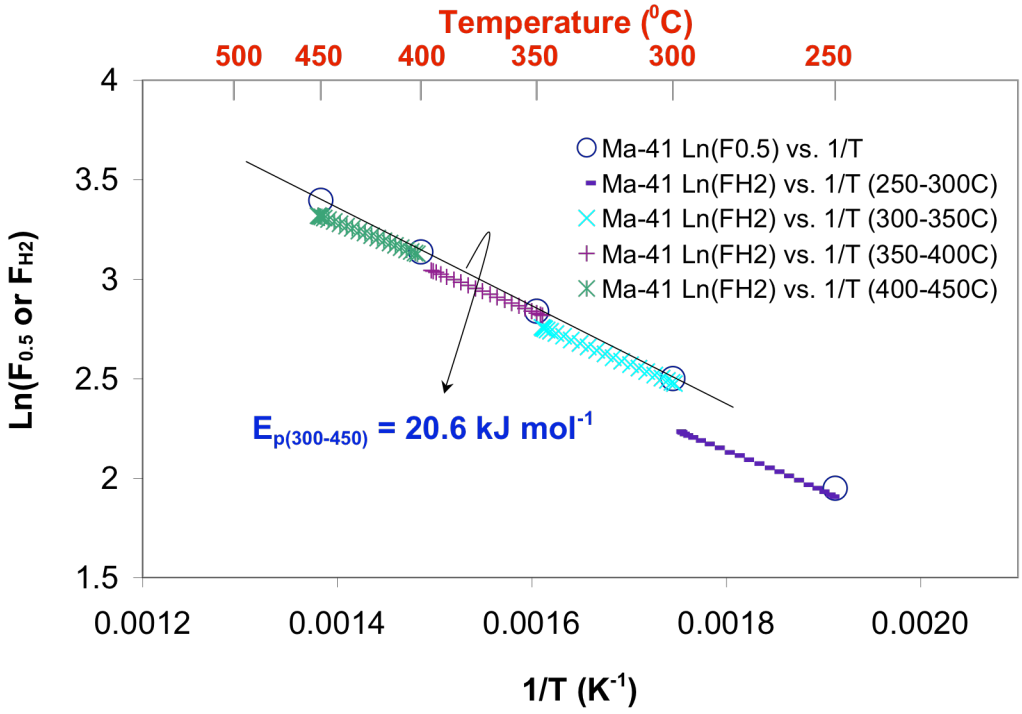

Figure 7-21 Arrhenius plot for membrane Ma-41. (open circles) permeance values $F_{0.5}$ from flux data in Figure 7-20.

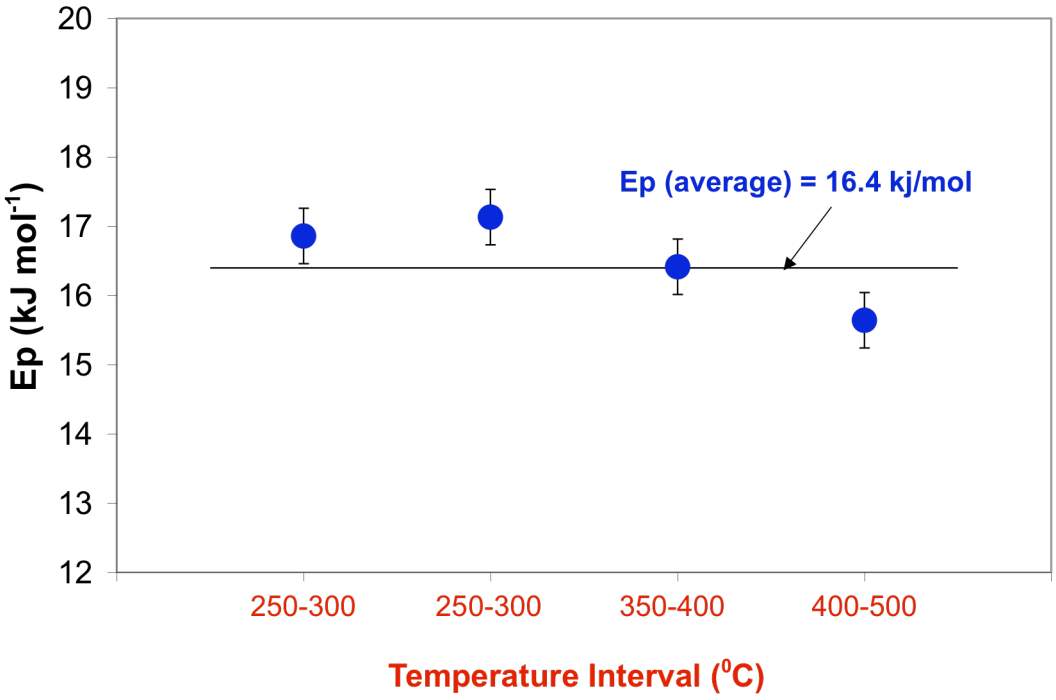

Figure 7-22 Activation energy for H_2 permeation for each temperature change.

The Cu content of membrane Ma-41 was estimated from the activation energy for H_2 permeation value. The average value of the E_p determined during each temperature change was equal to 16.4 kJ mol^{-1}. Figure 7-23 shows the activation energy for H_2 permeation for several PdCu alloys measured by Howard et al. (2004) in foils. The experimental data reported by Howard et al. (2004) was fitted with a 3rd degree polynomial function, which was equaled to 16.4 kJ mol^{-1} to solve for the Cu content in membrane Ma-41. A Cu content of around 7wt% was estimated as seen in Figure 7-23.

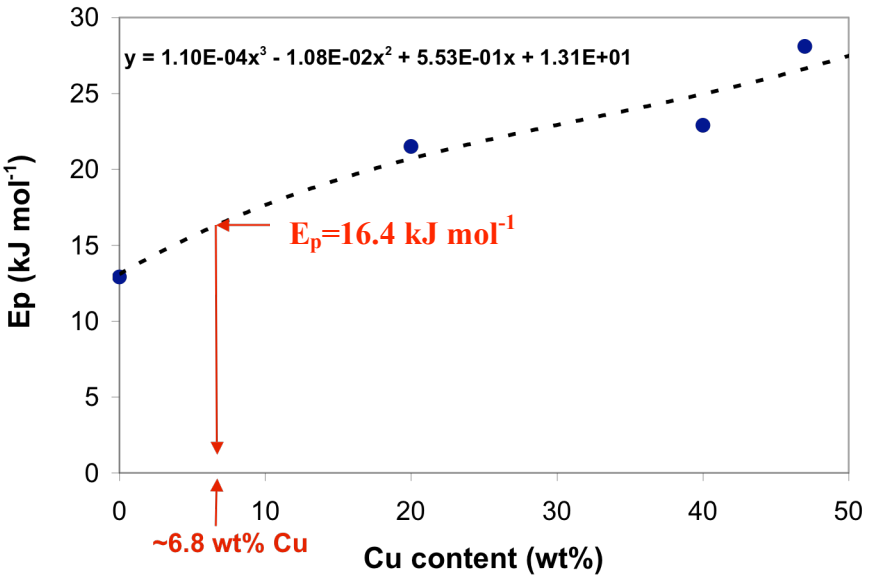

Figure 7-23 Activation energy for H_2 permeation in PdCu alloys as a function of Cu content.

7.5 Conclusions

Depending on the amount of Cu deposited on top of the Pd layer different phases appeared during the homogenization of the alloy. At low Cu loads only a Pd rich α phase was formed, at medium and high loads two phases were formed consisted of a Pd rich growing and a Cu rich dissolving phase. The transformation of α phase to β phase at a temperature of 400ºC was very fast. Indeed, the growth of the ordered β phase from the α phase only took 30 seconds. The formed phase was stable at temperatures lower than 525ºC. The preparation of a low Cu content Pd-Cu alloy membrane was possible on a graded PH support by the coating and diffusion method. The thin, 10μm, Pd-Cu membrane had a H_2 permeance as high as 30 $m^3/(m^2\ h\ bar^{0.5})$ at 450ºC and was stable for over 500 hr. The activation energy for H_2 permeation of Ma-41 was higher than the E_p of all other composite Pd membranes prepared on graded PH supports, in agreement with higher E_p for Pd-Cu alloys reported in the literature.